Chemical Science

ROYAL SOCIETY OF CHEMISTRY

EDGE ARTICLE

View Article Online
View Journal | View Issue

Cite this: *Chem. Sci.*, 2024, **15**, 16250

All publication charges for this article have been paid for by the Royal Society of Chemistry

Received 20th June 2024
Accepted 2nd September 2024

DOI: 10.1039/d4sc04056b

rsc.li/chemical-science

Cobalt-catalyzed conformationally restricted alkylarylation enables divergent access to Csp^3-rich N-heterocycles†

Kaixin Chen,‡[a] Jie Lin,‡[a] Jing Jing,[a] Junda Wang,[a] Jiayu Hu,[b] Hong Yi,*[b] Aiwen Lei*[b] and Jie Li*[a]

Due to the intrinsic spatial orientation and structural novelty, Csp^3-rich N-heterocycles have been recognized as increasingly sought-after scaffolds as compared to the aromatic ring-based moieties, which have generated considerable recent attention in drug discovery. Hence, we disclose a modular cobalt-catalyzed conformationally restricted alkylarylation strategy for the divergent access to Csp^3-rich N-hetero(spiro)cycles. Herein, multiple effects, including radical rebound and conformational restriction, play critical roles in the stabilization of the stereospecific alkyl-cobalt-aryl intermediate. Under simple and mild reaction conditions, cobalt catalyst combines a range of polyfunctionalized cyclenyl bromides and organozinc pivalates to rapidly and reliably forge the architecturally complex Csp^3-rich N-hetero(spiro)cycles (>70 examples, >20 : 1 dr), including but not limited to the [5,5]-, [5,6]-, [5,7]-, [5,12]-bicycles, tri- and tetracyclic N-heterocycles, as well as various novel N-heterospirocyclic scaffolds in one synthetic operation. Preliminary kinetic investigations suggested that the final reductive elimination might be the rate-determining step. Moreover, ample substrate scope, good functional group compatibility and facile derivatizations to the pharmaceutically active molecules show the potential applications of this technology to organic syntheses and drug discoveries in medicinal chemistry.

Introduction

Significant evidence proves that saturated and fused N-heterocyclic skeletons are important structural moieties due to their special three-dimensionality and rigidity, which can be commonly found in countless molecules of interest, including pharmaceuticals,[1] lead candidates and biologically active entities (Scheme 1a),[2] as well as organocatalysts (Scheme 1b).[3] Although many efforts have been made during the last decades, crucial drawbacks, such as the lack of stereoselectivity and generality in this area, exist.[4] Therefore, developing protocols that afford divergent polycyclic N-heterocycles in a stereocontrollable fashion is a longstanding goal in organic synthesis. Currently, Ru-NHC-catalyzed complete hydrogenation of indoles[5] under 100 bar of H_2 provides a platform to access octahydroindoles, while the relatively harsh conditions and the limited product type of [**5,6**]-fused N-heterocycles still represent drawbacks.

Considering that carbon–carbon bonds are the essential links in these Csp^3-riched N-heterocycles, the construction of carbon–carbon bonds is the key to building such scaffolds. Notably, transition metal-catalyzed dicarbofunctionalization of olefins has been recognized as an increasingly powerful tool to establish complex molecular architectures from simple chemical feedstocks *via* sequentially forging twofold C–C bonds. Among these methods, it is a significant challenge to prevent β-hydride elimination of the key Csp^3-[TM] intermediate. To this end, several strategies, such as radical rebound (**I**), substrate conjugation (**II**) and directing group chelation (**III**), as well as multiple effects operation in concert to enable the stabilization of Csp^3-[TM] intermediates for achieving dicarbofunctionalization of acyclic olefins have been recently developed.[6] However, representative drawbacks in controlling diastereoselectivity (strategies **A** and **B**) and pre-installation of directing groups (strategy **C**) still exist (Scheme 1c).

Recently, metal-catalyzed carboboration of endocyclic olefins has attracted considerable attention by offering considerable opportunities to the saturated (hetero)cyclic frameworks *via* conformational restriction strategy (**IV**),[7] mostly affording the thermodynamically favored isomers as

[a]*Key Laboratory of Organic Synthesis of Jiangsu Province, MOE Key Laboratory of Geriatric Diseases and Immunology, Suzhou Key Laboratory of Pathogen Bioscience and Anti-infective Medicine, College of Chemistry, Chemical Engineering and Materials Science, Soochow University, Suzhou 215123, China. E-mail: jjackli@suda.edu.cn*

[b]*College of Chemistry and Molecular Sciences, The Institute for Advanced Studies (IAS), Wuhan University, Wuhan, 430072, China. E-mail: hong.yi@whu.edu.cn; aiwenlei@whu.edu.cn*

† Electronic supplementary information (ESI) available. CCDC 2330506, 2330508, 2330499 and 2330494. For ESI and crystallographic data in CIF or other electronic format see DOI: https://doi.org/10.1039/d4sc04056b

‡ These authors contributed equally.

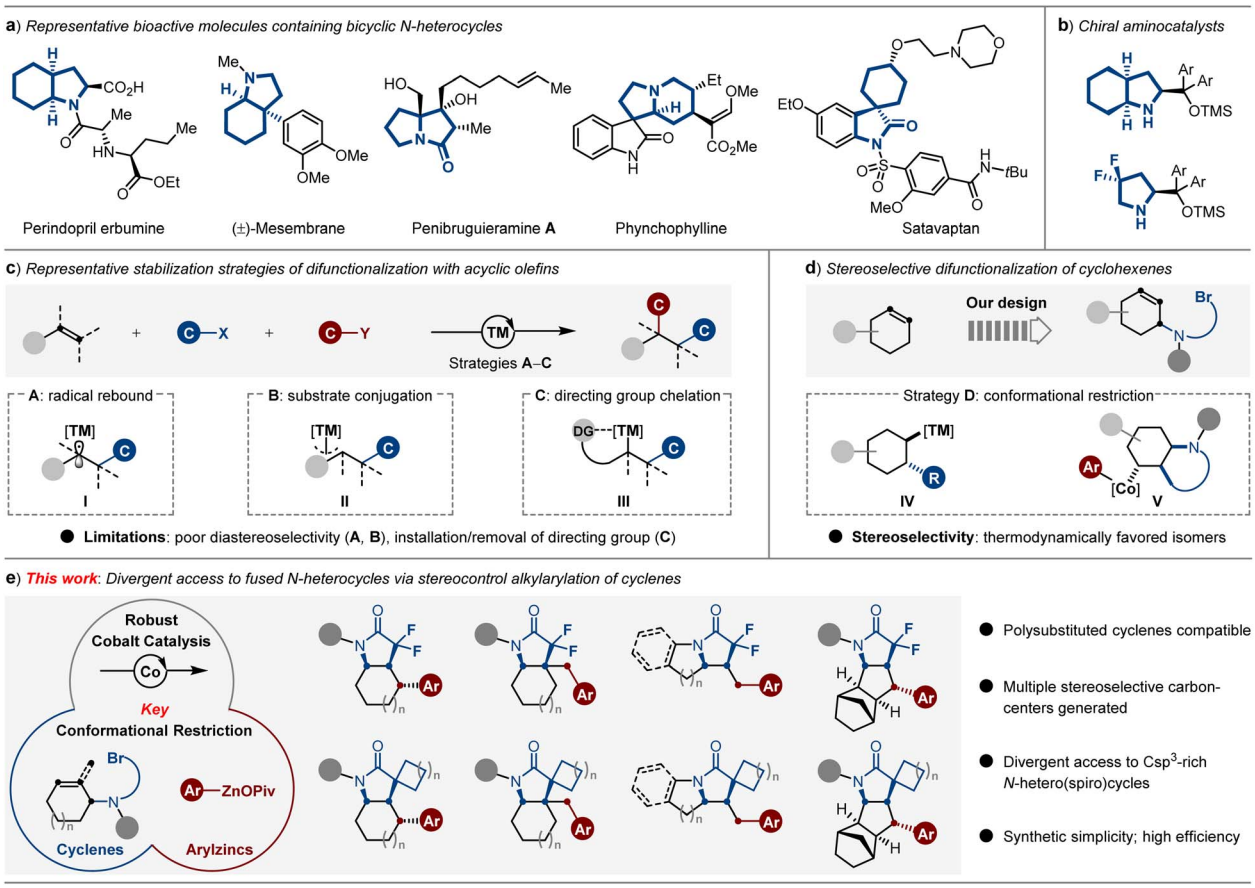

Scheme 1 Modular access to fused N-heterocycles *via* metal-catalyzed alkene difunctionalization strategy. (a) Representative biologically active molecules containing fused bicyclic N-heterocycles and (b) chiral aminocatalysts. (c) Working modes of metal-catalyzed dicarbofunctionalization of acyclic olefins. (d) Dicarbofunctionalization of cyclohexenes *via* conformational restriction. (e) Cobalt-catalyzed conformationally restricted alkylarylation enables divergent access to Csp^3-rich N-heterocycles.

the products (Scheme 1d, left).[8] Thus far, the substrate scope has largely been limited to the use of strained or activated endocyclic alkenes,[9] while the stereoselective dicarbofunctionalization of unactivated cyclenes still remains challenging.[10] Sporadic examples are shown to be highly dependent on the assistance of auxiliary directing groups.[11] Notably, a directing group-free nickel-catalyzed reductive dialkylation of endocyclic olefins was only recently disclosed by the Huang group, while the products were obtained in rather modest diastereoselectivity.[12]

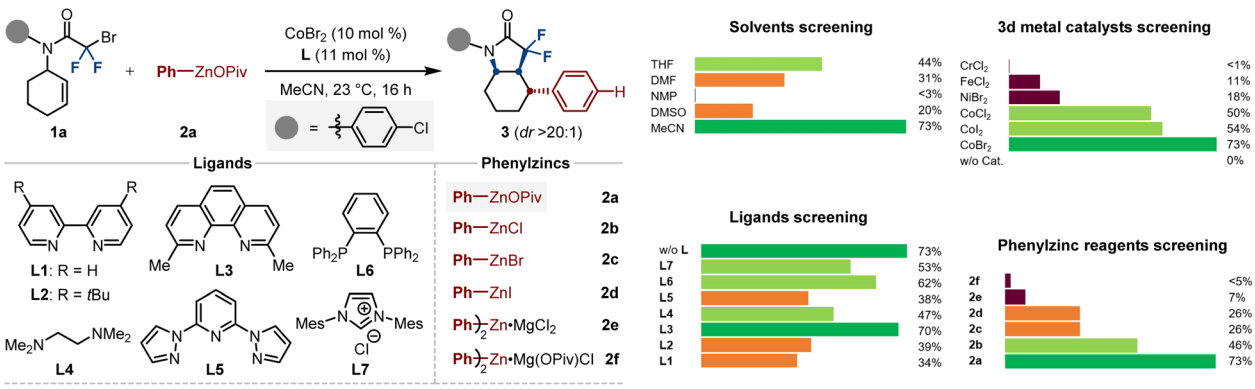

Fig. 1 Optimization for diastereoselective cobalt-catalyzed alkylarylation of cyclohexene (**1a**). Reaction conditions: **1a** (0.2 mmol, 1.0 equiv), **2a** (3.0 equiv), $CoBr_2$ (10 mol%), ligand (11 mol%), solvent (1.5 mL), 23 °C, 16 h. Yields are determined by GC analysis with dodecane as the internal standard.

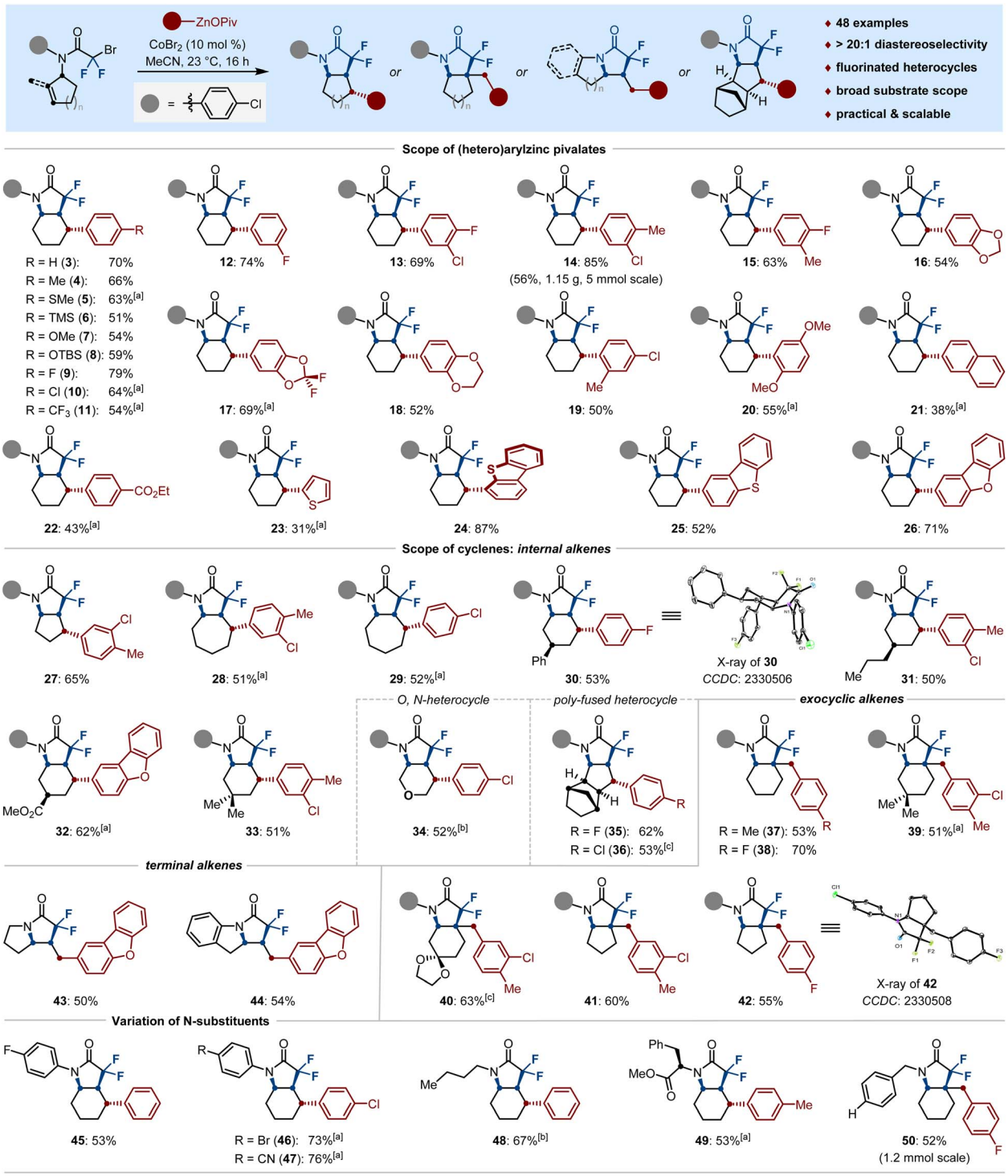

Scheme 2 Divergent access to fluorinated Csp^3-Rich N-heterocycles *via* cobalt-catalyzed difluoroalkylarylation. Reaction conditions: cyclenyl bromide (0.2 mmol, 1.0 equiv), (hetero)aryl–ZnOPiv (0.6 mmol, 3.0 equiv), $CoBr_2$ (10 mol%), MeCN (1.5 mL), 23 °C, 16 h. [a] **L3** (11 mol%) was used. [b] 0.1 mmol scale. [c] 0.15 mmol scale. High diastereoselectivity (dr > 20 : 1) for all the products was observed unless otherwise noted.

As a consequence, we believe that the dicarbofunctionalization of tethered cyclenes *via* the transition metal-catalyzed radical relay pathway involving the formation of a conformationally restricted intermediate, which will provide an attractive strategy for the rapidly divergent and stereoselective construction of fused Csp^3-rich N-heterocycles (Scheme 1d, right). Indeed, intramolecular cyclizations of tethered cyclenes *via* atom transfer radical addition (ATRA) could occur in the absence of transition metals. However, the synthesis of Csp^3-rich N-heterocycles bearing diverse carbogenic skeletons

through sequence C–C/C–C bond formation still has challenges.[13]

As such, our approach of achieving this goal is to design active catalysis that operates the cascade dicarbofunctionalization of tethered cyclenes in a stereoselective fashion. Recently, the dramatic paradigms of carboxylate-coordination[14] have been demonstrated in the preparation of solid organozinc pivalates,[15] which possess relatively attenuated reducibility and show the distinct advantage of reactivity among conventional organozinc halides in the 3d transition-metal-catalyzed radical relay cross-coupling reactions.[16] In this context, we detail the successful realization of divergent access to fused Csp^3-rich N-hetero(spiro)cycles through the development of a conformationally restricted alkylarylation of cyclenes with readily available solid (hetero)arylzinc pivalates using industrially-friendly cobalt catalyst.[17] Keys to our success of this strategy are the multiple effects of radical rebound and conformational restriction, which efficiently avoids the facile β-hydride elimination process, thus forming the stereospecific intermediate **V**. Under the optimal reaction conditions, the cobalt catalyst combines a range of polyfunctionalized cyclenyl bromides and organozinc pivalates to rapidly and reliably forge the architecturally complex Csp^3-rich N-hetero(spiro)cycles with structural, functional, and physical features in medicinal chemistry (Scheme 1e).

Results and discussion

We began our studies by evaluating the cobalt-catalyzed diastereoselective alkylarylation of cyclohexene (**1a**) with salt-stabilized phenylzinc pivalate (**2a**). Preliminary experiments identified MeCN as the ideal reaction solvent and $CoBr_2$ as the metal source of choice, which gave the arylated *cis*-octahydroindol-2-one **3a** in 70% isolated yield with excellent diastereoselectivity (Fig. 1, top). Notably, to further examine the efficacy of cobalt catalysis, various chelating ligands such as bis(pyridine)s (**L1–3**), TMEDA (**L4**), tridentate 2,6-bis(*N*-pyrazolyl)pyridine (**L5**), dppbz (**L6**) and N-heterocyclic carbene (**L7**), could not lead to further increased yield; only neocuproine (**L3**) afforded the desired product **3a** with equal efficiency to the former ligand-free conditions. With these results in hand, we wondered whether the high efficacy of this cobalt-catalyzed alkylarylation process was dominated by the phenylzinc pivalate. Hence, a series of different phenylzincs **2b–2f** were prepared through transmetallation of Ph–MgCl (1.0 equiv) with corresponding ZnX_2 (1.2 or 0.5 equiv; X = OPiv, Cl, Br, I). Thereafter, we tested their reactivity in the diastereoselective cobalt-catalyzed alkylarylation by parallel experiments. Notably, as compared to the solid Ph–ZnOPiv (**2a**),[18] the other different phenylzinc halides **2b–2d**, as well as the diphenylzincs **2e–2f**, had a deleterious effect on the cobalt catalysis, thereby

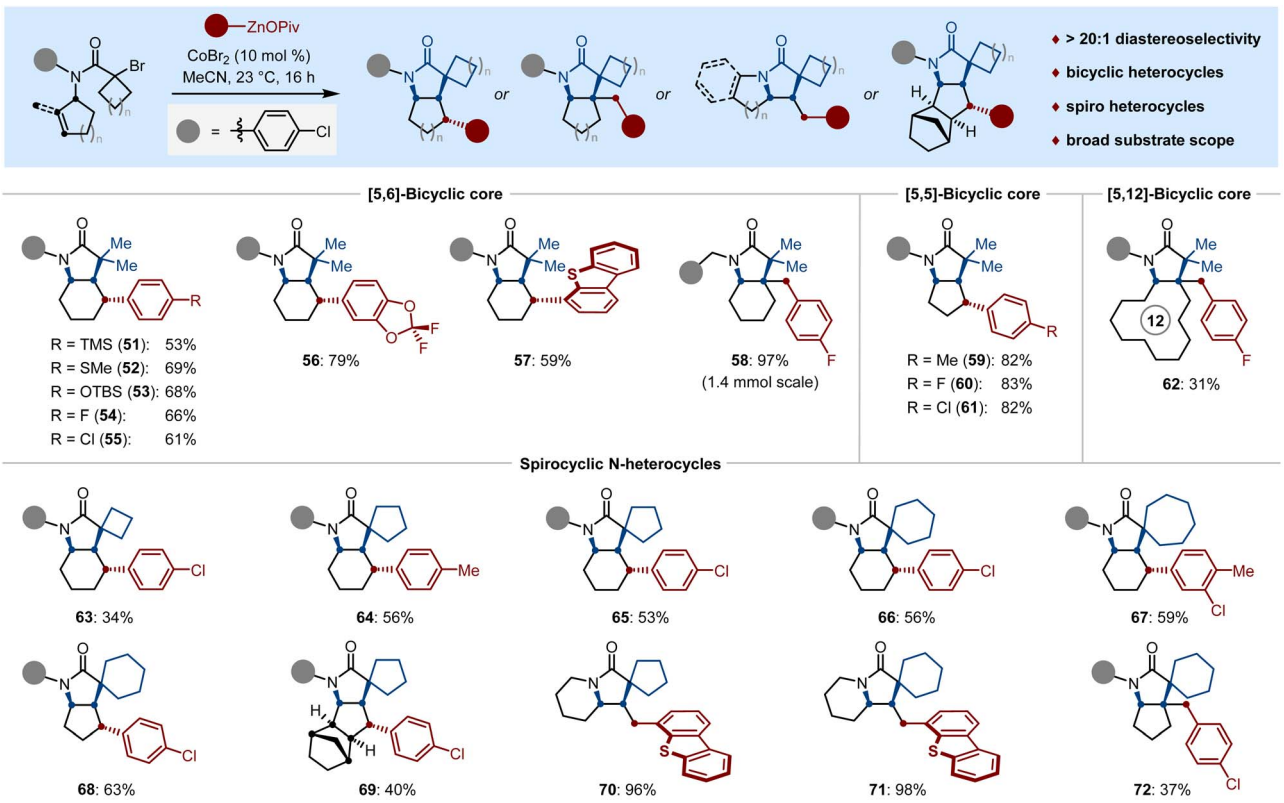

Scheme 3 Modular access to fused N-heterocycles and N-spirocycles *via* cobalt-catalyzed alkylarylation. Reaction conditions: cyclenyl bromide (0.2 mmol, 1.0 equiv), (hetero)aryl–ZnOPiv (0.6 mmol, 3.0 equiv), $CoBr_2$ (10 mol%), MeCN (1.5 mL), 23 °C, 12 h. High diastereoselectivity (dr > 20 : 1) for all the products was observed unless otherwise noted.

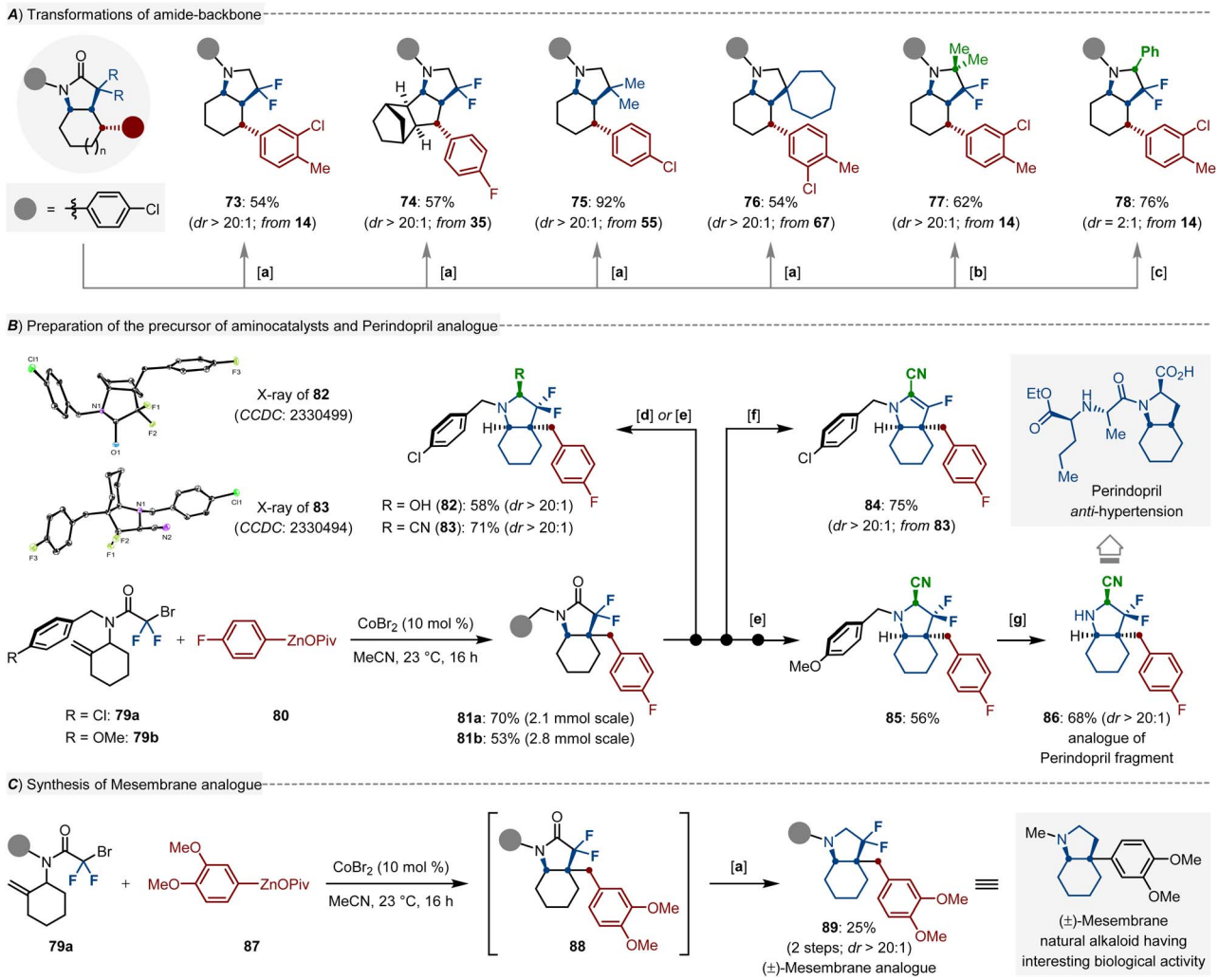

Scheme 4 Synthetic applications. (A) Functionalization of amide-backbones, (B) late-stage synthesis of medicinally relevant molecules, (C) preparation of analogue of mesembrane. Reaction conditions: [a] $Mn(CO)_5Br$ (2.0 mol%), Ph_2SiH_2 (2.0 equiv), THF, 80 °C, 4 h. [b] MeLi (1.0 equiv), $TiCl_4$ (1.0 equiv), and MeLi (2.0 equiv), Toluene. [c] (i) NaH (3.0 equiv), NaI (1.0 equiv), THF, 40 °C, 3 h; (ii) TMSCl (2.5 equiv), PhMgCl (2.0 equiv), 0 to 23 °C, 2 h. [d] (i) NaH (3.0 equiv), NaI (1.0 equiv), THF, 70 °C, 16 h; (ii) TMSCl (4.0 equiv), Bu_4NCN (2.0 equiv), 23 °C, 5 h. [e] (i) DIBAL (1.3 equiv), THF, −35 °C, 2 h; (ii) TMSCN (5.0 equiv), −35 to 20 °C, 1 h. [f] (i) KOH (2.0 equiv) in H_2O, 1,4-Dioxane, 115 °C, 3 h; (ii) then HCl. [g] TFA, anisole, 55 °C, 2 h.

considerably restraining the desired reaction to occur. This observation is particularly noteworthy, as it suggests that the anion-coordination in organozinc pivalates promotes the catalytic activity of cobalt catalysts (Fig. 1).

With the optimal reaction conditions established, we next turned our attention to examining the versatility of our stereoselective difluoroalkylarylation of cyclenes. As shown in Scheme 2, the scope of arylzinc pivalates (**3–22**) was largely insensitive to electronic and steric variations at the *para*-, *meta*-, and *ortho*-positions of appropriately aryl-substituted nucleophiles. Indeed, various functional groups such as SMe (**5**), TMS (**6**), OTBS (**8**), F (**9**, **12**, **13**, **15**), Cl (**10**, **13**, **14**, **19**), CF_3 (**11**), dioxole (**16–18**) and ester (**22**) were well tolerated under the cobalt catalysis, furnishing the N-heterocycles in moderate to high yields with excellent stereoselectivity. Notably, our protocol could be extended to the construction of thiophene-, (di)benzothiophene- and (di)benzofuran-based backbones (**23–26**) when employing the corresponding solid heteroarylzinc pivalates as the nucleophilic partners; the structure of **25** was further validated by single-crystal X-ray diffraction. Furthermore, the current difluoroalkylarylation reaction can be conducted with a wide range of cyclenes. The ring size of the cyclic alkenes had no significant influence on the catalytic efficacy and five- and seven-membered olefins were well difluoroalkylarylated with arylzinc pivalates, leading to the bicyclic pyrrolidones **27–29** in 51%–65% yields. Gratifyingly, side chains of cyclohexene possessing phenyl (**30**), *n*-propyl (**31**), ester (**32**) and bismethyl (**33**) substituents posed no problem, thereby delivering the tetra-substituted cyclohexanes in a stereoselective manifold. Among them, the spatiotemporal selectivity of **30** was confirmed by single-crystal X-ray diffraction.

Interestingly, the O-based cyclohexene, as well as the fused cyclopentene could be stereoselectively coupled to afford the novel N-heterocyclic scaffolds **34–36** in 52%–62% yields. As

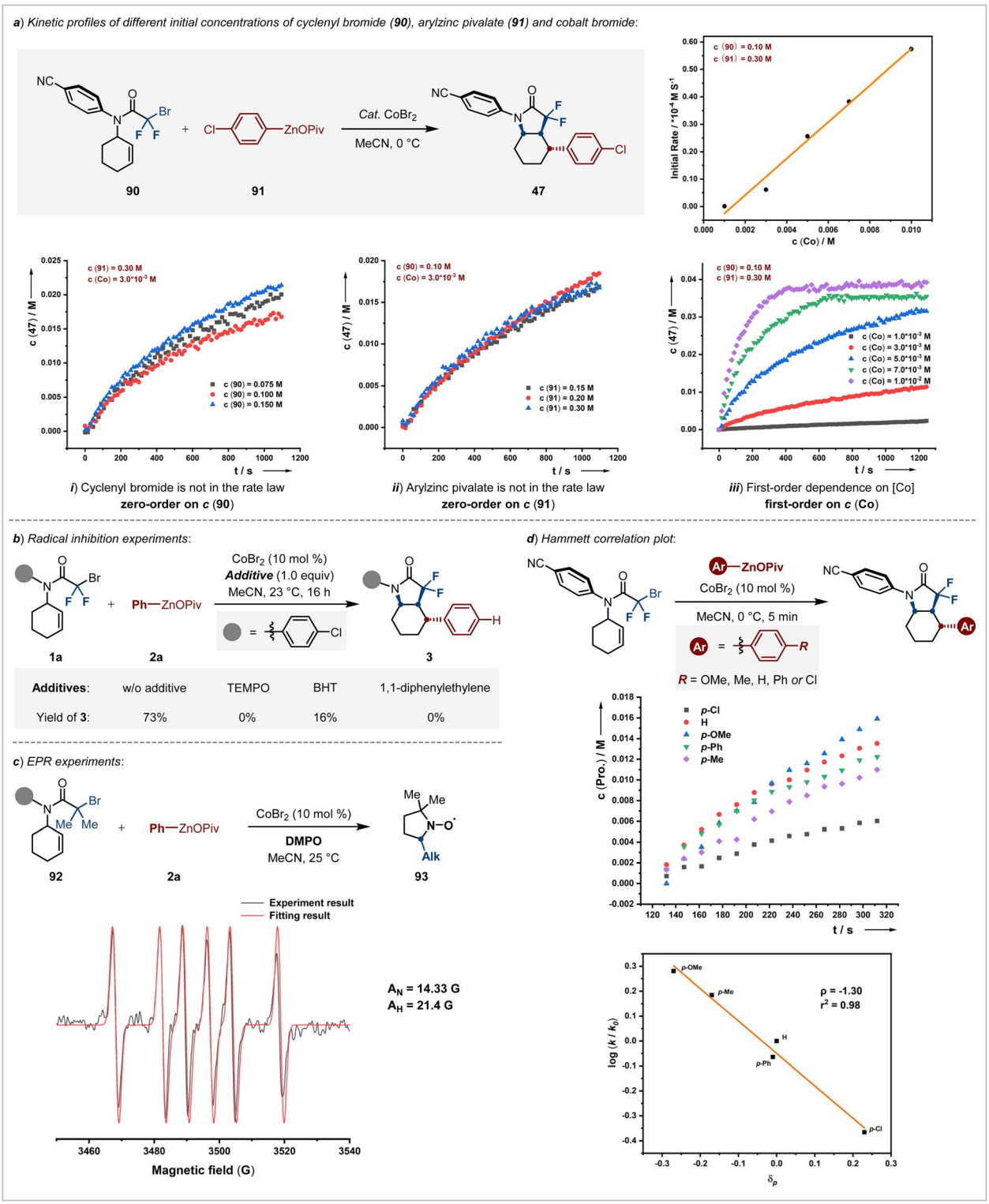

Scheme 5 Mechanistic studies. (a) Kinetic profiles, (b) radical inhibition experiments, (c) EPR experiments and (d) Hammett correlation plot with different arylzinc pivalates.

shown for **37–42**, the reactions could be further extended to the more challenging exocyclic alkenes to generate the bicyclic N-heterocycles *via* building an all-carbon quaternary center and following Csp^3–Csp^2 bond formation with arylzinc pivalates. Remarkably, the pyrrolizines and their derivatives, which are important structural motifs of alkaloids with activities of relevance to biology or medicinal chemistry,[2d,19] are easily within reach under identical reaction conditions; the desired

fluorinated N-heterocycles **43–44** were obtained in 50–54% yields. Beyond that, a variation of the substitution pattern on the nitrogen atom was also investigated, such as aliphatic chain (**48**), removable benzyl group (**50**), as well as arenes bearing fluoro (**45**), sensitive bromo (**46**) and nitrile (**47**) functional groups, which proved to be suitable substrates. Even phenylalanine (**49**) could be aryl-bicyclized in satisfied yield with remarkably high diastereoselectivity.

Encouraged by the successful preparation of fluorinated bi-, tri-and tetracyclic N-heterocycles, we wondered whether it would be possible to enable a cyclized alkylarylation of the non-fluorinated cyclenyl bromides (Scheme 3). Substrates containing tertiary alkyl bromide resulted in stereoselective dicarbofunctionalization with various functionalized arylzinc pivalates, affording the [**5**,**6**]-, and [**5**,**5**]-bicyclic N-heterocycles **51–61** in 53%–97% yields with excellent diastereoselectivity (dr > 20 : 1). Interestingly, a 12-membered exocyclic alkene was proven to be a viable substrate as well, which smoothly underwent cyclized alkylarylation to afford the [**5**,**12**]-fused bicyclic heterocycle **62** bearing a quaternary center, albeit in a modest yield. Driven by the prevalence of N-heterospirocyclic motifs in a myriad of natural products and biologically relevant compounds,[2a] we were pleased to find that our protocol could be also effective for the divergent synthesis of spirocyclic pyrrolidinones **63–72** in one step *via* a facile spirocyclized alkylarylation, thus allowing us to dictate the site- and diastereoselective incorporation of the (hetero)aryl moiety at β-Csp^3 sites within a spirocyclic N-heterocycle.

In addition, the lactam backbone of the resulting products could be easily subjected to the facile manganese-catalyzed deoxygenation using Ph_2SiH_2 as the reductant, the high-valued amines **73–75** and spirocyclic amine **76** were obtained in 54–92% yields. Notably, catalytic hydrogenation of indoles could not afford these scaffolds.[5] Moreover, both MeLi and PhMgCl are suitable nucleophiles for the one-pot sequential reductive dimethylation (**77**) or arylation (**78**) processes (Scheme 4A). To further illustrate the synthetic versatility of our protocol in organic synthesis, large-scale reaction with **79** performed under the standard reaction conditions, and the resulting [**5**,**6**]-bicyclic lactam **81** successfully underwent stereoselective functionalization to afford the hydroxylated (**82**) and cyanated (**83**) products in a diastereoselective manifold, the stereoscopic conformation was validated by X-ray diffraction. Upon treatment of **83** with a stoichiometric amount of KOH, a monofluorinated product **84** was obtained in 75% yield. Moreover, we removed the protecting group of **85** to obtain a [**5**,**6**]-bicyclic amine **86**, which is the analogue of the perindopril fragment (Scheme 4B). To access the mesembrane analogue **89** we devised a two-step reaction sequence consisting of the cobalt-catalyzed diastereoselective cyclic alkylarylation, along with manganese-catalyzed deoxygenation, which set the stage for the efficient preparation of the natural alkaloids, again with excellent regio- and diastereoselectivity (Scheme 4C).

Following the evaluation of the scope and applications, we sought to disclose to unveil the underlying mechanism of the reaction. Our exploration began with a thorough kinetic analysis of diastereoselective cobalt-catalyzed cyclic alkylarylation coupling reactions performed in MeCN at 0 °C (Scheme 5a). Notably, when we varied the initial concentrations of cyclenyl bromide **90**, the reaction rates remained nearly unchanged, indicating that the alkylarylation process does not depend on the concentration of cyclenyl bromide. These observations suggested the halogen atom abstraction *via* single-electron transfer from a cobalt catalyst is not the rate-limiting step. Similarly, altering the concentrations of arylzinc pivalate **91** did not considerably affect the reaction rates, reinforcing our understanding of the reaction dynamics (Scheme 5a-ii). However, a linear increase in the reaction rate with increasing concentrations of the [Co] catalyst was observed, pointing to a first-order dependence on the [Co] catalyst. Therefore, the above kinetic findings highlighted that reductive elimination might be the rate-determine step.[20]

Further evidence supporting our mechanistic hypothesis came from control experiments using stoichiometric amounts of radical scavengers. These additives dramatically reduced the yield of the desired product **3** or completely halted the reaction (Scheme 5b), consistent with the results from EPR spin-trapping experiments. The detection of a carbon-centered radical intermediate **93** ($g = 2.006$, $A_N = 14.33$ G, $A_H = 21.4$ G), captured by 5,5-dimethyl-1-pyrroline *N*-oxide (DMPO), confirms the radical's role in the reaction pathway.[21]

To delve deeper insights into the influence of electronic effects on the transmetallation step, we employed Hammett correlation analysis (Scheme 5d). A negative ρ value (−1.30) revealed that the aryl-cobalt species behaves as a nucleophile, with electron-donating groups on arylzinc pivalates, enhancing the nucleophilicity of aryl-cobalt. This interaction facilitates the reaction with the *in situ* generated alkyl radical, shedding light on intricate electronic interactions governing this step.

On the basis of the above observations and previous insights,[16a,c] we proposed the catalytic cycle involves an initial intermolecular halogen atom transfer from alkyl bromide to the low-valent active species Co(I) **A**, thereby affording a Co(II) intermediate **C** and liberating an alkyl radical **B**. Subsequently, transmetallation reaction between **C** and arylzinc pivalate delivered the arylcobalt species **E**, while the alkyl radical **B**

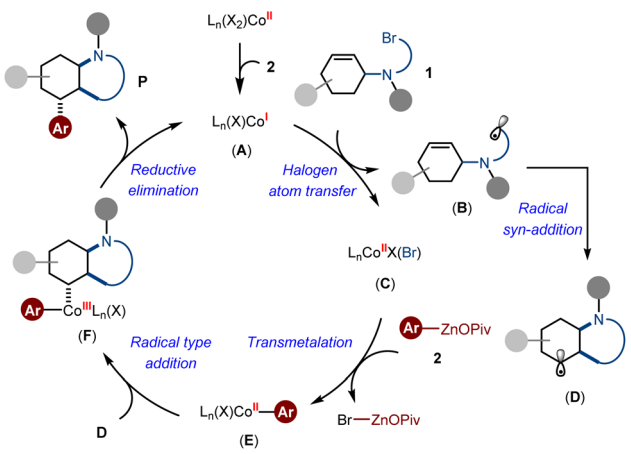

Scheme 6 Proposed catalytic cycle.

underwent intramolecular *syn*-addition to generate the intermediate **D**. At this stage, the dramatic effects of radical rebound and conformational restriction dominated the formation of intermediate **F** in a diastereoselective fashion. Finally, the reductive elimination process of **F** gave the desired Csp^3-rich N-heterocycles as the products (Scheme 6).

Conclusions

In conclusion, we have documented a general, divergent cobalt-catalyzed domino cyclized alkylarylation of cyclenes, which enabled the construction of up to seven stereocenters. This method afforded a broad range of highly valuable Csp^3-rich N-heterocycles and spirocyclic pyrrolidinones in good yields and diastereoselectivities. It is worth emphasizing that the newly formed cyclic alkyl radical features high stereospecific control, thereby undergoing conformational restriction strategy with the *in situ* formed aryl-cobalt nucleophile. Preliminary kinetic experiments suggested that the reductive elimination step might be the rate-limiting step. Moreover, the salient features of our protocol are the synthetic simplicity, wide scope and mild reaction conditions. The great potential of this protocol was illustrated by accessing the analogues of medicinally relevant molecules and aminocatalysts. We believe that this methodology will complement and expand the area of metal-catalyzed cascade radical relay cross-couplings and provide an efficient synthetic route to the preparation of Csp^3-rich N-hetero(spiro)cycles, which are likely to be attractive in fragment-based lead identification projects.

Data availability

The datasets supporting this article have been uploaded as parts of the ESI materials.† Crystallographic data for the structures reported in this article have been deposited at the Cambridge Crystallographic Data Centre, under deposition numbers CCDC 2330506 (**30**), 2330508 (**42**), 2330499 (**82**), and 2330494 (**83**). Copies of the data can be obtained free of charge *via* **www.ccdc.cam.ac.uk/structures**.

Author contributions

J. L. conceived and directed the project and wrote the manuscript by all the other authors; K. C., J. Lin developed and performed the catalytic methods and the synthetic applications. H. Y., and A. L. designed and directed the mechanistic studies; K. C., and J. H. performed the mechanistic studies; K. C., J. J., and J. W. prepared the starting materials, all the authors were involved in the interpretation of the results presented in the manuscript.

Conflicts of interest

There are no conflicts to declare.

Acknowledgements

We thank the National Natural Science Foundation of China (22322108), Natural Science Foundation of Jiangsu Province (BK20231521, BK20221355) and Jiangsu Specially Appointed Professors Plan (SR10900122) for generous financial supports. We are grateful to Prof. Konstantin Karaghiosoff (Ludwig-Maximilians-Universität München) for his help in X-ray crystal analysis.

Notes and references

1 (*a*) M. Hurst and B. Jarvis, *Drugs*, 2001, **61**, 867–896; (*b*) D. N. Tran, A. Zhdanko, S. Barroso, P. Nieste, R. Rahmani, J. Holan, R. Hoefnagels, P. Reniers, F. Vermoortele, S. Duguid, L. Cazanave, M. Figlus, C. Muir, A. Elliott, P. Zhao, W. Paden, C. H. Diaz, S. J. Bell, A. Hashimoto, A. Phadke, J. A. Wiles, I. Vogels and V. Farina, *Org. Process Res. Dev.*, 2022, **26**, 832–848; (*c*) C. Pascard, J. Guilhem, M. Vincent, G. Remond, B. Portevin and M. Laubie, *J. Med. Chem.*, 1991, **34**, 663–669; (*d*) A. Kleemann, J. Engel, B. Kutscher and D. Reichert, *Pharmaceutical Substances*, Thieme, Stuttgart, 4th edn, 2001, pp. 1785–1787.

2 (*a*) K. Hiesinger, D. Dar'in, E. Proschak and M. Krasavin, *J. Med. Chem.*, 2021, **64**, 150–183; (*b*) P. Bhutani, G. Joshi, N. Raja, N. Bachhav, P. K. Rajanna, H. Bhutani, A. T. Paul and R. Kumar, *J. Med. Chem.*, 2021, **64**, 2339–2381; (*c*) Y. Zheng, C. M. Tice and S. B. Singh, *Bioorg. Med. Chem. Lett.*, 2014, **24**, 3673–3682; (*d*) S. Bindra, in *The Alkaloids*, ed. R. H. F. Manske, Academic Press, New York, 1973, pp. 84–121.

3 (*a*) M. Berger, D. Ma, Y. Baumgartner, T. H.-F. Wong and P. Melchiorre, *Nat. Catal.*, 2023, **6**, 332–338; (*b*) E. Arceo, I. D. Jurberg, A. Álvarez-Fernández and P. Melchiorre, *Nat. Chem.*, 2013, **5**, 750–756.

4 (*a*) W. R. Bowman, M. O. Cloonan and S. L. Krintel, *J. Chem. Soc., Perkin Trans. 1*, 2000, 1–14; (*b*) C. V. Galliford and K. A. Scheidt, *Angew. Chem., Int. Ed.*, 2007, **46**, 8748–8758; (*c*) V. B. Phapale, E. Buñuel, M. García-Iglesias and D. J. Cárdenas, *Angew. Chem., Int. Ed.*, 2007, **46**, 8790–8795; (*d*) M. Kamlar, M. Urban and J. Veselý, *Chem. Rec.*, 2023, **23**, e202200284.

5 F. Zhang, H. S. Sasmal, C. G. Daniliuc and F. Glorius, *J. Am. Chem. Soc.*, 2023, **145**, 15695–15701.

6 Selected reviews and examples:(*a*) Y.-C. Luo, C. Xu and X. Zhang, *Chin. J. Chem.*, 2020, **38**, 1371–1394; (*b*) J. Diccianni, Q. Lin and T. Diao, *Acc. Chem. Res.*, 2020, **53**, 906–919; (*c*) J. Derosa, O. Apolinar, T. Kang, V. T. Tran and K. M. Engle, *Chem. Sci.*, 2020, **11**, 4287–4296; (*d*) R. Giri and S. Kc, *J. Org. Chem.*, 2018, **83**, 3013–3022; (*e*) R. K. Dhungana, S. KC, P. Basnet and R. Giri, *Chem. Rec.*, 2018, **18**, 1314–1340; (*f*) J.-W. Gu, Q.-Q. Min, L.-C. Yu and X. Zhang, *Angew. Chem., Int. Ed.*, 2016, **55**, 12270–12274; (*g*) C. Xu, R. Cheng, Y.-C. Luo, M.-K. Wang and X. Zhang, *Angew. Chem., Int. Ed.*, 2020, **59**, 18741–18747; (*h*) J. Derosa, V. A. van der Puyl, V. T. Tran, M. Liua and K. M. Engle, *Chem. Sci.*, 2018, **9**, 5278–5283; (*i*) J. Derosa, T. Kang, V. T. Tran, S. R. Wisniewski, M. K. Karunananda, T. C. Jankins, K. L. Xu and K. M. Engle, *Angew. Chem., Int. Ed.*, 2020, **58**, 1202–1205; (*j*) L. Liu, W. Lee, C. R. Youshaw, M. Yuan, M. B. Geherty, P. Y. Zavalij and O. Gutierrez,

Chem. Sci., 2020, **11**, 8301–8305; (*k*) A. García-Domínguez, R. Mondal and C. Nevado, *Angew. Chem., Int. Ed.*, 2019, **58**, 12286–12290; (*l*) S. Kc, R. K. Dhungana, N. Khanal and R. Giri, *Angew. Chem., Int. Ed.*, 2020, **59**, 8047–8051; (*m*) J. Wang, D. Luo, Y. Hu, Z. Duan, J. Yao, K. Karaghiosoff and J. Li, *Sci. China: Chem.*, 2024, **67**, 360–367; (*n*) D. Wang and L. Ackermann, *Chem. Sci.*, 2022, **13**, 7256–7263; (*o*) H.-Q. Ni, P. Cooper, S. Yang, F. Wang, N. Sach, P. G. Bedekar, J. S. Donaldson, M. Tran-Dubé, I. J. McAlpine and K. M. Engle, *Angew. Chem., Int. Ed.*, 2022, **61**, e202114346.

7 (*a*) K. M. Logan, S. R. Sardini, S. D. White and M. K. Brown, *J. Am. Chem. Soc.*, 2018, **140**, 159–162; (*b*) S. Joung, A. M. Bergmann and M. K. Brown, *Chem. Sci.*, 2019, **10**, 10944–10947; (*c*) C. Ding, Y. Ren, C. Sun, J. Long and G. Yin, *J. Am. Chem. Soc.*, 2021, **143**, 20027–20034; (*d*) Y. Li, Y. Li, H. Shi, H. Wei, H. Li, I. Funes-Ardoiz and G. Yin, *Science*, 2022, **376**, 749–753; (*e*) W. Kong, Y. Bao, L. Lu, Z. Han, Y. Zhong, R. Zhang, Y. Li and G. Yin, *Angew. Chem., Int. Ed.*, 2023, **62**, e202308041; (*f*) G. L. Trammel, P. B. Kannangara, D. Vasko, O. Datsenko, P. Mykhailiuk and M. K. Brown, *Angew. Chem., Int. Ed.*, 2022, **61**, e202212117.

8 (*a*) H. Ohmiya, H. Yorimitsu and K. Oshima, *J. Am. Chem. Soc.*, 2006, **128**, 1886–1889; (*b*) T. Thaler, B. Haag, A. Gavryushin, K. Schober, E. Hartmann, R. M. Gschwind, H. Zipse, P. Mayer and P. Knochel, *Nat. Chem.*, 2010, **2**, 125–130; (*c*) T. Thaler, L.-N. Guo, P. Mayer and P. Knochel, *Angew. Chem., Int. Ed.*, 2011, **50**, 2174–2177; (*d*) J. Li, Q. Ren, X. Cheng, K. Karaghiosoff and P. Knochel, *J. Am. Chem. Soc.*, 2019, **141**, 18127–18135.

9 (*a*) L. Dian, D. S. Müller and I. Marek, *Angew. Chem., Int. Ed.*, 2017, **56**, 6783–6787; (*b*) H. Li, M. Zhang, H. Mehfooz, D. Zhu, J. Zhao and Q. Zhang, *Org. Chem. Front.*, 2019, **6**, 3387–3391; (*c*) A. A. Kadam, T. L. Metz, Y. Qian and L. M. Stanley, *ACS Catal.*, 2019, **9**, 5651–5656; (*d*) S. KC, R. K. Dhungana, N. Khanal and R. Giri, *Angew. Chem., Int. Ed.*, 2020, **59**, 8047–8051; (*e*) Y. Ito, S. Nakatani, R. Shiraki, T. Kodama and M. Tobisu, *J. Am. Chem. Soc.*, 2022, **144**, 662–666.

10 S. Teng, Y. R. Chi and J. S. Zhou, *Angew. Chem., Int. Ed.*, 2021, **60**, 4491–4495.

11 (*a*) C. Xu, R. Cheng, Y.-C. Luo, M.-K. Wang and X. Zhang, *Angew. Chem., Int. Ed.*, 2020, **59**, 18741–18747; (*b*) V. Aryal, L. J. Chesley, D. Niroula, R. R. Sapkota, R. K. Dhungana and R. Giri, *ACS Catal.*, 2022, **12**, 7262–7268; (*c*) M.-K. Wang, Y.-C. Luo, H.-Y. Zhao, Y. Zhang, D. Zhang and X. Zhang, *ACS Catal.*, 2023, **13**, 14090–14102.

12 C. Rao, T. Zhang, H. Liu and H. Huang, *Nat. Catal.*, 2023, **6**, 847–857.

13 (*a*) B. Giese, B. Kopping, T. Gobel, J. Dickhaut, G. Thoma, K. J. Kulicke and F. Trach, *Org. React.*, 1996, **48**, 301–856; (*b*) S. Z. Zard, *Radical Reaction in Organic Synthesis*, Oxford University Press, New York, 2003, selected examples; (*c*) G. Storke and R. Mah, *Heterocycles*, 1989, **28**, 723–727; (*d*) D. J. Babcock, A. J. Wolfram, J. L. Barney, S. M. Servagno, A. Sharma and E. D. Nacsa, *Chem. Sci.*, 2024, **15**, 4031–4040; (*e*) C.-J. Wallentin, J. D. Nguyen, P. Finkbeiner and C. R. J. Stephenson, *J. Am. Chem. Soc.*, 2012, **134**, 8875–8884.

14 A. Hernán-Gómez, E. Herd, E. Hevia, A. R. Kennedy, P. Knochel, K. Koszinowski, S. M. Manolikakes, R. E. Mulvey and C. Schnegelsberg, *Angew. Chem., Int. Ed.*, 2014, **53**, 2706–2710.

15 (*a*) S. Bernhardt, G. Manolikakes, T. Kunz and P. Knochel, *Angew. Chem., Int. Ed.*, 2011, **50**, 9205–9209; (*b*) C. I. Stathakis, S. Bernhardt, V. Quint and P. Knochel, *Angew. Chem., Int. Ed.*, 2012, **51**, 9428–9432; (*c*) S. M. Manolikakes, M. Ellwart, C. I. Stathakis and P. Knochel, *Chem.–Eur. J.*, 2014, **20**, 12289–12297; (*d*) J. Wang, Z. Duan, X. Liu, S. Dong, K. Chen and J. Li, *Angew. Chem., Int. Ed.*, 2022, **61**, e202202379.

16 (*a*) X. Cheng, X. Liu, S. Wang, Y. Hu, B. Hu, A. Lei and J. Li, *Nat. Commun.*, 2021, **12**, 4366; (*b*) J. Lin, K. Chen, J. Wang, J. Guo, S. Dai, Y. Hu and J. Li, *Chem. Sci.*, 2023, **14**, 8672–8680; (*c*) X. Liu, H. Chen, D. Yang, B. Hu, Y. Hu, S. Wang, Y. Lan, A. Lei and J. Li, *ACS Catal.*, 2023, **13**, 9254–9263.

17 (*a*) A. Guérinot and J. Cossy, *Acc. Chem. Res.*, 2020, **53**, 1351–1363; (*b*) J. Li, *Top. Organomet. Chem.*, 2023, **71**, 113–144; (*c*) F. H. Lutter, S. Graßl, L. Grokenberger, M. S. Hofmayer, Y.-H. Chen and P. Knochel, *ChemCatChem*, 2019, **11**, 5188–5197; (*d*) G. Cahiez and A. Moyeux, *Chem. Rev.*, 2010, **110**, 1435–1462; (*e*) C. Gosmini, J.-M. Bégouin and A. Moncomble, *Chem. Commun.*, 2008, 3221–3233.

18 Note: Ar–ZnOPiv•Mg(OPiv)X is abbreviated henceforth as Ar–ZnOPiv (X = Cl, Br, or I) for the sake of clarity.

19 T. Aniszewski, Definition, Typology and Occurrence of Alkaloids, in *Alkaloids-Secrets of Life*, Elsevier, Amsterdam, 2007, pp. 1–59.

20 (*a*) L. Jin, H. Zhang, P. Li, J. R. Sowa Jr and A. Lei, *J. Am. Chem. Soc.*, 2009, **131**, 9892–9893; (*b*) C. He, J. Ke, H. Xu and A. Lei, *Angew. Chem., Int. Ed.*, 2013, **52**, 1527–1530.

21 W.-M. Cheng, R. Shang and Y. Fu, *Nat. Commun.*, 2018, **9**, 5215.